

Kinematic & Dynamic Simulation Of A 2d Aerospace Structure for Esa -Lagard Project

Evangelos Kaslis¹, Dimitrios E. Mazarakos¹, Andreas Ampatzoglou¹,
Dimitrios E. Vlachos² and Vassilis Kostopoulos¹

¹ Department of Mechanical Engineering and Aeronautics, University of Patras, Rio Campus 22500, Greece

² Adamant Composites Ltd, Platani 22500, Greece

Corresponding Author: Dimitrios E. Mazarakos

-----ABSTRACT-----

In this survey, the kinematic-dynamic analysis of a 2D deployable truss (both rigid and flexible body analysis) is presented. This deployable truss is the main part of an octagonal 9-bay space deployable structure that was developed during ESA-LAGARD Project. The scope of the structure is the accommodation of parts of a space telescope for future ESA science missions. The functional specifications demand high stiffness and accuracy in the fully deployed configuration. The truss is consisted of CFRP beams, connected with rigid titanium connectors. The truss is actuated by a fully motorized mechanism controlled by electric step motors. For each bay, longerons members are rotated around a hinge point leading to the translation of a frame of batten elements. This movement leads to the 9-bay octagonal structure's deployment. The kinematic - dynamic analysis task is critical for the design, as it is necessary for the motorization subsystem's sizing process. A rigid body approach was proposed for the truss's kinematic and dynamic response using analytical formulas in order to verify the numerical models in MSC ADAMS. The truss's flexibility and deformations were further investigated combining FE models. The results were used during the preliminary design phase in order to build the testing plan procedure for the full-scale structure securing the normal operation.

KEYWORDS;- Space telescopes; Deployable structures; Kinematic and Dynamic analysis; ADAMS

Date of Submission: 01-12-2021

Date of Acceptance: 15-12-2021

I. INTRODUCTION

During the last decades, there is a necessity in the astrophysics and astronomy scientific community for deep space investigation tools. Space telescopes are the main tools that are used for this role. X-ray and Gamma ray telescopes are used to capture high-resolution deep space images. The operating principle of such telescopes (due to high photons energetic nature) has lead the engineers to design high focal length telescopes, meaning telescopes with focal length up to tens of meters. The simplest and most efficient solution to achieve such focal length levels in space is to employ deployable structures with a low packaging ratio (Conley et al, 1998).

The most popular engineering concepts in the field of deployable space structures-masts are ADAM (NASA, USA) (Figure 1a) and HALCA (JAXA, Japan) (Figure 1b) (Puig and Rando, 2010), (Santiago and Baier, 2013), Chu et al. ,2014). The ESA-LAGARD project set out to develop a European version for a modular deployable mast. This project is lead by Adamant Composites Ltd (Prime Contractor, Greece) and UPat Applied Mechanics Laboratory (Partner-subcontractor, Greece). This paper addresses the necessary kinematic and dynamic analyses performed for a2D module, which is the basic unit of the full structure. The load cases provided with valuable information for the estimation of 2D module dynamic/structural behavior during deployment phase, the motors' power consumption and loads on the titanium connectors. These data were extrapolated for the design and analysis process of the full 3D LAGARD Structure.

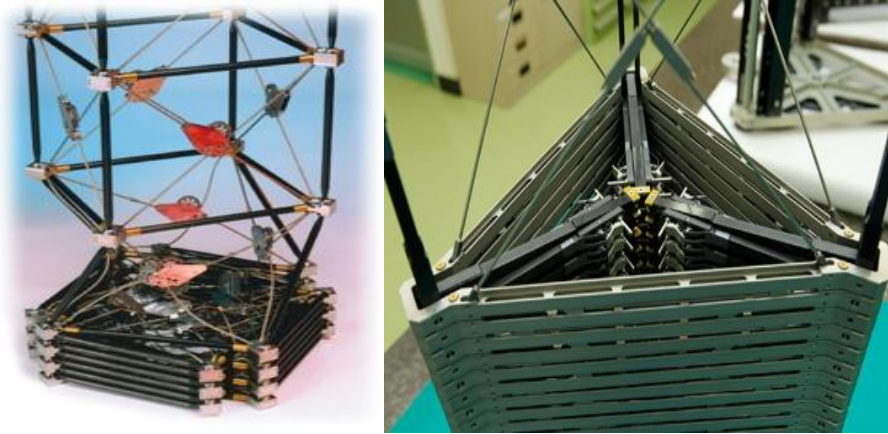


Figure 1: Aerospace Deployable Structures, left: ADAM Mast (NASA, USA) & Right: HALCA Mast (JAXA, Japan)

II. DESCRIPTION OF 3D DEPLOYABLE TRUSS STRUCTURE – 2D BASIC MODULE

The deployable structure-mast is a 3D truss and it is consisted of 2D repetitive frames around the main structure. The 2D frame is the basic module of the 3D deployable mast. This module is placed peripherally and longwise in order to build a 9-bay octagonal 3D mast (Figure 2) which supports the X-Ray/Gamma-Ray telescopes.

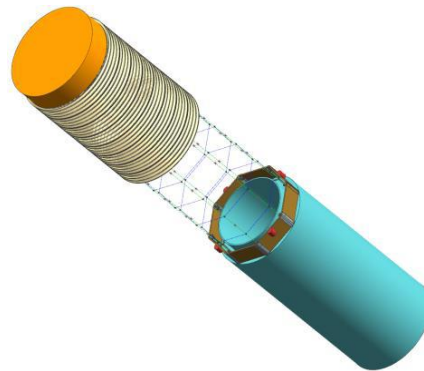


Figure 2: 2 Nine-bay octagonal 3D mast

The 2D basic module is scalable and modular structure following the launch carrier's space accommodation and the aerospace industries' certifications. The 3D deployable mast's main functional specifications are presented in **Error! Reference source not found.:**

Table 1: LAGARD Structure main functional specifications

Specifications	Limitations
Deployment length	Between 11 m and 21 m
Package ratio	Less than 10%
Coefficient of Thermal Expansion	Less than $5e-6$
Total mass	Less than Length x Diameter x 12 kg/m^2
Stability Ratio in Operation	Less than $10e-4$
First Bending eigen frequency	Greater than 1 Hz
Operational temperature	Between $-10 \text{ }^\circ\text{C}$ and $30 \text{ }^\circ\text{C}$
Survival temperature	Between $-60 \text{ }^\circ\text{C}$ and $60 \text{ }^\circ\text{C}$
Launch environment and attachments	Ariane 5

The final layout for the 2D basic module and 3D deployable mast (the first stage only) relative to the requirements is presented in Figure 3. The selected materials (carbon tubes for struts, CFRP cables and titanium connectors) and their mechanical properties are included in **Error! Reference source not found.**

Table 2: Struts and connectors mechanical properties

Pultruded strut: T700/Epoxy	
E_{11} (GPa)	140
E_{22} (GPa)	12.1
E_{33} (GPa)	12.1
G_{12} (GPa)	4.4
G_{13} (GPa)	4.4
G_{23} (GPa)	3.2
ν_{12}	2.48e-1
ν_{13}	2.48e-1
ν_{23}	4.58e-1
ρ (kg/m ³)	1610
Connectors: Titanium	
E (GPa)	113.8
ν	0.342
Cable: CFRP	
E (GPa)	126.4
ν	0.35

For the motorization subsystem, the step motors (GPL 052-2S/41.6.1) were the main selection as a primary device for the deployment of the 3D truss structure. The actuation subsystem is consisted of 8 pins (one at each corner of the truss) which are moved linearly on a ball screw powered by the step motors. A system of levers engages the 2D module assisting to the normal deployment.

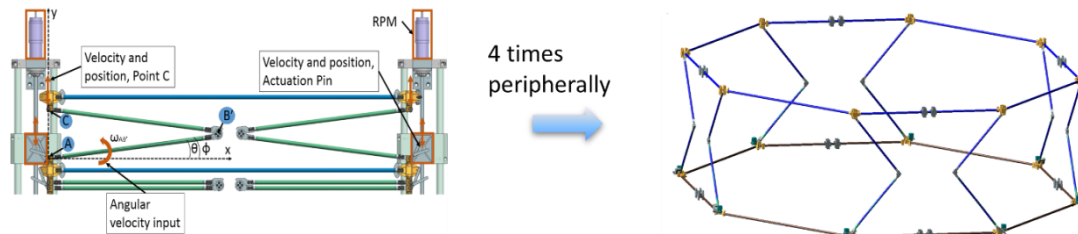


Figure 3: Semi -deployed 2D truss and One-bay semi-deployed 3D truss

III. KINEMATIC AND DYNAMIC ANALYSIS (2D FRAME)

A mathematical model was set, describing the 2D Truss kinematics and Dynamics motion. The model was necessary in order to calculate the actuation force/torque for the truss motors. The mathematical model includes the geometrical data, the mass/ inertia properties and the external loads and calculates the necessary torque and angular velocity for actuation. These input data are parameters for the mathematical model in order to calculate the output results.

Geometrical model:

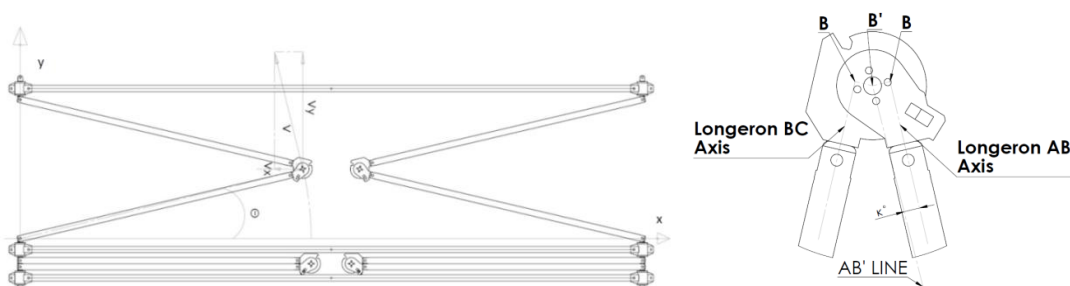


Figure 4: 2D Truss geometry and connector's details, (left) 2D Truss geometry actuation velocities, (right) Connection detail: Rotation points

The basic 2D module is presented in Figure 4. The actuation can be introduced with 2 different options: a) With force F_{act} at the longerons' connections (joint B')-Scenario 1 and b) with torque M_{act} at the longeron /batten connection (joint A)-Scenario 2. The two velocity components (V_x , V_y) are the result from the

motorization system's actuation. The harness material is also included in the model and there are two different scenarios: a) the harness's mass and inertia is distributed on the longerons/batten geometry and b) the harness mass and inertia is simply concentrated and applied as force on joint C. As these scenarios are more specific, a generic Kinematic/Dynamic mathematical model was established including all the crucial parameters in order to estimate the response and the actuation forces/torque in various conditions and design loads.

Mathematical model (kinematics/ Dynamics)

Only the half (symmetry plane yz) 2D basic module is investigated. Due to the symmetry, only the left part was considered taking into account: the functionality of the mechanism the symmetric plane internal loads and reaction forces. (The coordination system for the mathematical model is similar to the geometrical model, x-i/ y-j).

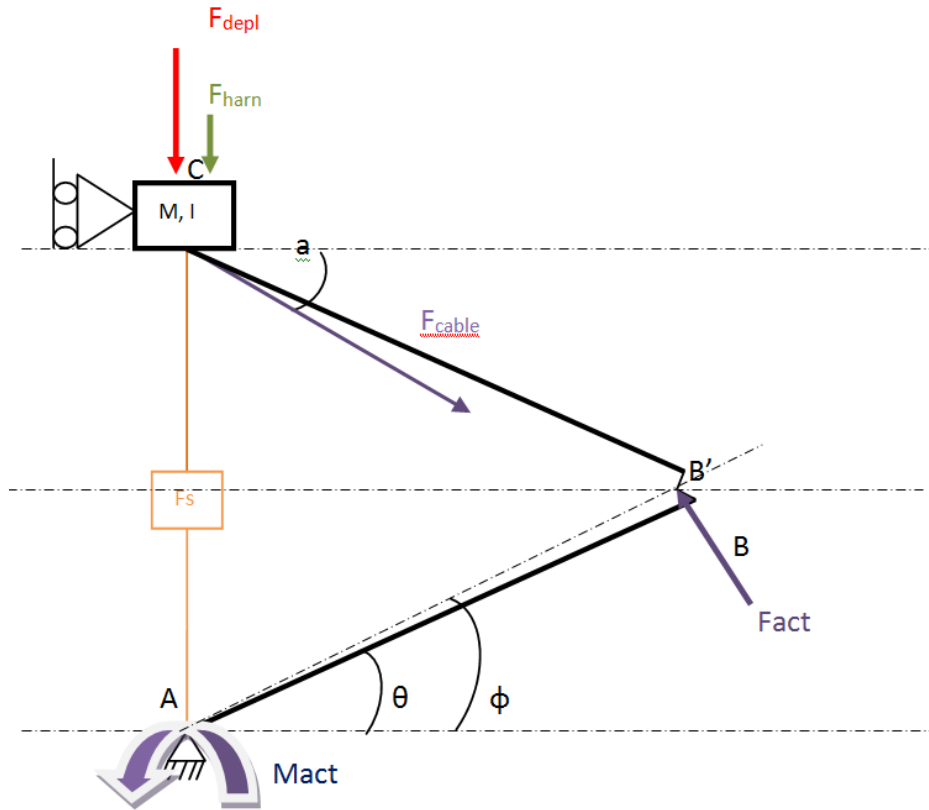


Figure 5: Equivalent kinematics and dynamics mathematical model for the symmetry plane of the 2D truss

For the main scenario (scenario 1), the actuation torque M_{act} is introduced at the joint A by the motor. In the secondary scenario (scenario 2), the force F_{act} is applied at the point B' by the motor. The actuation length AB' is the distance between the point A (rotation point) and the actuation point B'. The point B' is just above the B point. The angle between the x-axis and the AB' is ϕ , and is calculated by: $\phi = \theta + \kappa$, where κ is a constant value. A mathematical transformation is used between ϕ and θ in order to calculate the actuation torque and the reaction forces. The mathematical model assists the comparison between the main and secondary scenario, providing information for the forces/moments and the reaction loads on the joints.

The calculations are based on the Newton's second law for linear and rotary motion (dynamics) and the geometry (kinematics). The reaction forces, the velocities and accelerations on truss's pins are calculated regarding the input data.

The angular position of the longeron (θ) and its angular velocity ω_{AB} are input data for the system's motion. The longeron's angular position is described by the equation $\theta = \phi - \kappa$.

The angular acceleration is α_{AB} the first derivative of the angular velocity so,

$$\alpha_{AB} = \frac{d}{dt} \omega_{AB} \quad (1)$$

It is also valid that, $\omega_{AB} = \omega_{AB'}$, (2) $\omega_{BC} = \omega_{B'C}$ (3) and $\omega_{AB} = -\omega_{BC}$, (4) $\alpha_{AB} = -\alpha_{BC}$ (5)

$$a = \frac{d}{dt} \omega_{AB} = \frac{d}{dt} \left(\frac{V_{XB'}(t)}{L_{AB'} * \frac{H}{L_{AB'}}} \right) = \frac{d}{dt} \left(\frac{V_{XB'}(t)}{H} \right)$$

$$= \frac{a_{GABx} * H - V_{XB'}(t) * V_{YB'}(t)}{H^2} \quad (6)$$

$$a_{GBCx} = a_{AB} * Y_{B'} + \omega_{AB}^2 * X_{B'} + a_{BC} * Y_{GBC} - a_{BC} * Y_{B'} + \omega_{BC}^2 * X_{GBC} - \omega_{BC}^2 * X_{B'} \quad (7)$$

$$a_{GBCy} = a_{AB} * X_{B'} + \omega_{AB}^2 * Y_{B'} + a_{BC} * X_{GBC} - a_{BC} * X_{B'} + \omega_{BC}^2 * Y_{GBC} - \omega_{BC}^2 * Y_{B'} \quad (8)$$

$$a_{Cy} = a_{AB} * X_{B'} + \omega_{AB}^2 * Y_{B'} - a_{BC} * X_{B'} + \omega_{BC}^2 * Y_C - \omega_{BC}^2 * Y_{B'} \quad (9)$$

The reaction forces at the point B (Bx and By) are given by:

$$B_x = F_c \cos \alpha + R_{cx} - m_{BC} * a_{GBCx} \quad (10)$$

$$B_y = m * a_{Cy} - F_s - F_c \sin \alpha - m * g - m_{BC} * g - m_{BC} * a_{GBCy} - F_{depl} - F_{HARNESS} \quad (11)$$

The actuation Torque and Force are respectively :

$$M_{act} = I_A * a_{AB} - B_y * X_{B'} + B_x * Y_{B'} + M_{AD} + M_{BD} - m_{AB} * a_{GABy} * L_{GAB} * \cos \theta - m_{AB} * a_{GABx} * L_{GAB} * \sin \theta + m_{AB} * g * L_{GAB} * \sin \theta + M_{A,HARNESS} + M_{B,HARNESS} \quad (12)$$

or

$$F_{act} = \frac{1}{L_{AB'}} * (I_A * a_{AB} - B_y * X_{B'} + B_x * Y_{B'} + M_{AD} + M_{BD} - m_{AB} * a_{GABy} * L_{GAB} * \cos \theta - m_{AB} * a_{GABx} * L_{GAB} * \sin \theta + m_{AB} * g * L_{GAB} * \sin \theta + M_{A,HARNESS} + M_{B,HARNESS}) \quad (13)$$

The reaction forces at the point A are:

$$A_x = F_{act} \sin \varphi - B_x - m_{AB} * a_{GABx} \quad (14)$$

$$A_y = m_{AB} * a_{GABy} + m_{AB} * g - B_y - F_s - F_{act} \cos \varphi \quad (15)$$

$$a_{GABx} = a_{AB} * Y_{GAB} + \omega_{AB}^2 * X_{GAB} \quad (16)$$

$$a_{GABy} = a_{AB} * X_{GAB} + \omega_{AB}^2 * Y_{GAB} \quad (17)$$

The total velocity at point B' ($V_{B'}$) is function of the angular velocity and the angle φ . So,

$$V_{XB'} = \omega_{AB} * L_{AB'} * \sin \varphi \quad (18)$$

$$V_{YB'} = \omega_{AB} * L_{AB'} * \cos \varphi \quad (19)$$

The rigid body analysis of the 2D module's components (longerons, buttens etc.) were incorporated in a MATLAB code including all the necessary data for each part (inertia, mass, dimensions etc.) in order to run multi parametric analysis. In addition, a combined methodology was developed in order to calibrate the MSC ADAMS numerical results for rigid body analysis and expanding these calculations for the flexible body analysis.

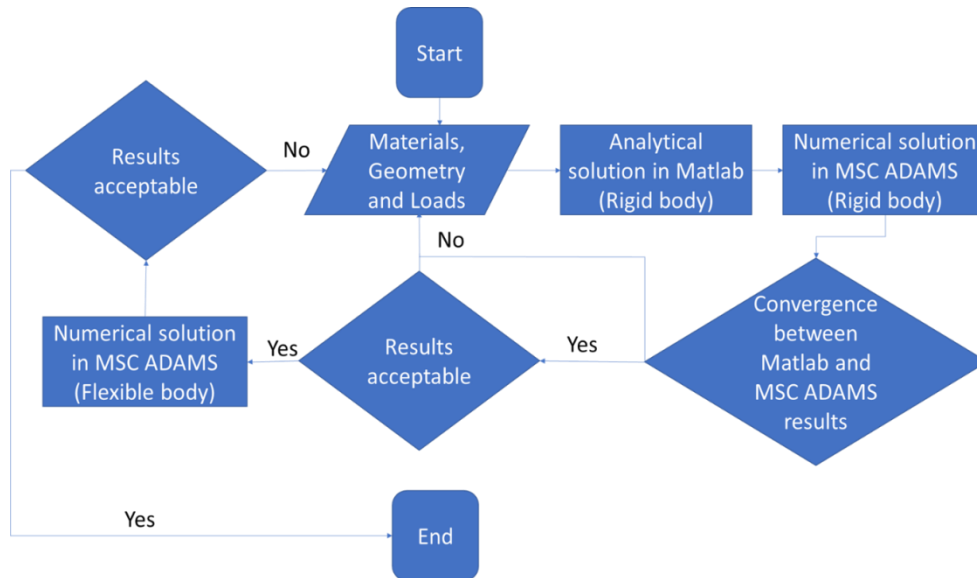


Figure 6: Design flow chart for MSC ADAMS software and MATLAB code comparisons

In this survey, a full run for a torque actuated 2D module (scenario 1) is presented. The basic input data and the calculations are included in **Error! Reference source not found.**. The deployment is a time dependent process and it is based on the linear velocity of the upper batten. The time parameter was included in all the time dependent variables, creating an iterative process in MATLAB (Moore, 2015). In each time step, the output values (necessary actuation torque, reaction forces at A & B) are calculated relative to the input data (Butten linear velocity)

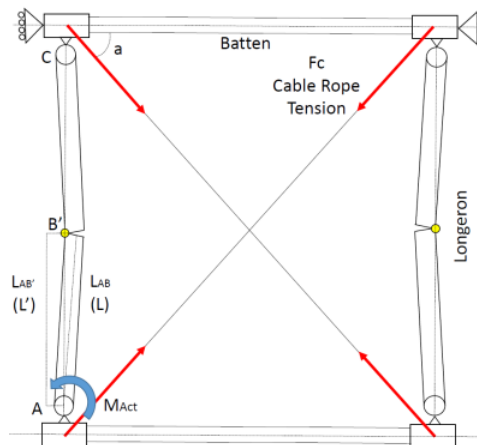


Figure 7 : Basic kinematic/dynamic model for the 2D basic module

Table 3: Basic kinematic/dynamic input/output data of the 2D module’s response for the Scenario 1

Time allocation for deployment: 1800seconds
For the X-Ray: 9 bays, approximately 210seconds per bay
The total velocity at point B’ ($V_{B'}$) is function of the input velocities $V_{xB'}$, $V_{yB'}$:
$V_{xB'} = \omega_{AB} L_{AB'} \sin\phi$
$V_{yB'} = \omega_{AB} L_{AB'} \cos\phi$
From the above equations, the angle ϕ is given by:
$\phi = \tan^{-1} \left(\frac{V_{xB'}}{V_{yB'}} \right)$, and the angular velocity ω_{AB} is calculated.
Also, $\theta = \phi - k$
The angular acceleration, α_{AB} is derived from the angular velocity:
$\alpha_{AB} = \frac{d}{dt} \omega_{AB}$
It is also valid that, $\omega_{AB} = -\omega_{BC}$ and $\alpha_{AB} = -\alpha_{BC}$

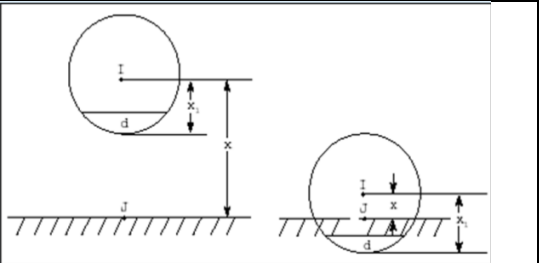
$a_{AB} = \frac{d}{dt} \omega_{AB} = \frac{d}{dt} \left(\frac{V_{XB}(t)}{L_{AB} \cdot \sin(\theta(t))} \right) =$ $= - \frac{2 * V_{XB}(t) * \theta'(t) * \sin(\theta(t)) * \sin(2 * \theta(t))}{L_{AB} * (\cos(2 * \theta(t)) - 1)^2} - \frac{2 * \sin(\theta(t)) * V_{XB}'(t)}{L * (\cos(2 * \theta(t)) - 1)} =$ $= - \frac{2 * V_{XB}(t) * \omega_{AB}(t) * \sin(\theta(t)) * \sin(2 * \theta(t))}{L_{AB} * (\cos(2 * \theta(t)) - 1)^2} - \frac{2 * \sin(\theta(t)) * a_{XB}(t)}{L * (\cos(2 * \theta(t)) - 1)}$	
Linear acceleration in the x direction of the center of mass (CoM) of Longeron B'C	
$a_{GBCx} = a_{AB} * Y_{B'} + \omega_{AB}^2 * X_{B'} + a_{BC} * Y_{GBC} - a_{BC} * Y_{B'} + \omega_{BC}^2 * X_{GBC} - \omega_{BC}^2 * X_{B'}$	
Linear acceleration in the y direction of the center of mass (CoM) of Longeron B'C	
$a_{GBCy} = a_{AB} * X_{B'} - \omega_{AB}^2 * Y_{B'} + a_{BC} * X_{GBC} - a_{BC} * X_{B'} - \omega_{BC}^2 * Y_{GBC} + \omega_{BC}^2 * Y_{B'}$	
Linear acceleration in the y direction of point C	
$a_{Cy} = a_{AB} * X_{B'} - \omega_{AB}^2 * Y_{B'} + a_{BC} * X_{GBC} - a_{BC} * X_{B'} - \omega_{BC}^2 * Y_{GBC} + \omega_{BC}^2 * Y_{B'}$	
Linear acceleration in the x direction of the center of mass (CoM) of Longeron AB'	
$a_{GABx} = a_{AB} * Y_{GAB} + \omega_{AB}^2 * X_{GAB}$	
Linear acceleration in the y direction of the center of mass (CoM) of Longeron AB'	
$a_{GABy} = a_{AB} * X_{GAB} + \omega_{AB}^2 * Y_{GAB}$	
$Y_C = 2 * L_{AB'} * \sin\varphi$	Position of point C, Y-axis, (m)
$Y_{B'} = L_{AB'} * \sin\varphi$	Position of point B', Y-axis, (m)
$X_{B'} = L_{AB'} * \cos\varphi$	Position of point B', X-axis, (m)
$X_{GBC} = L_{GBC} * \cos\theta$	CoG of member BC, X-axis, (m)
$Y_{GBC} = Y_C - L_{GCB} * \sin\theta$	CoG of member BC, Y-axis, (m)
$L = L_{CB'} * \cos\varphi - L_{GCB} * \cos\theta$	
$H = L_{CB'} * \sin\varphi - L_{GCB} * \sin\theta$	
$a = \text{atan} \left(\frac{Y_c}{L_{bat}} \right)$	Cable angle a (rad)
Gravity field g=0 m/s^2	Deep space operation and deployment simulation

The MATLAB code with analytical equations for the 2D module's kinematics and dynamics was further used for the calibration of the contact elements at MSC ADAMS. Having the same input file (batten's linear velocity), a numerical model in MSCADAMS was developed in order to simulate the 2D module's motion and include flexibility effects at the latter stage. For the linear velocity input profile at point C (**Error! Reference source not found.**), the MSC ADAMS contact settings (**Error! Reference source not found.**) were estimated in order to avoid penetration and rebound forces using the following equation (MSC Software,2016):

$$Contact\ force = \begin{cases} Max(0, k(x_1 - x)^e - STEP(x, x_1 - d, c_{max}, x_1, 0))\dot{x} : x < x_1 \\ 0 : x \geq x_1 \end{cases} \quad (20)$$

Table 3: MSC-ADAMS contact parameters for rigid body modeling

Parameter	Value
Distance between two objects, x	Default
Relative velocity between two objects, \dot{x}	Default
Trigger distance, x_1	Default
Stiffness coefficient, k (N/m)	1e+10
Stiffness force exponent, e	2.2
Damping Coefficient, c_{max} . (N*s/m)	1e+8
Damping ramp up distance, d (m)	1e-4



The input velocity profile is an important factor for the analysis in order to have a normalized motion without acceleration and jerk peaks. These peaks could create impact forces preventing the 2D basic module's functionality.

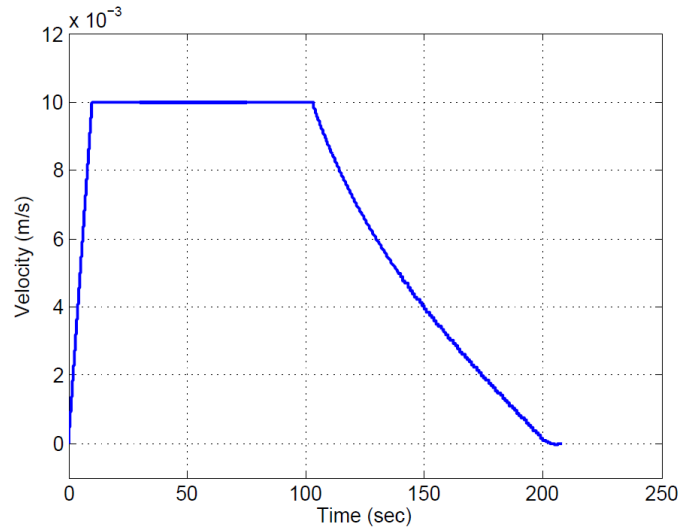


Figure 8: Linear Velocity (v_{Cy}) versus time for point C

The results for the comparisons between MATLAB rigid body code and MSC-ADAMS rigid model analysis after the calibration are presented in Figure 9

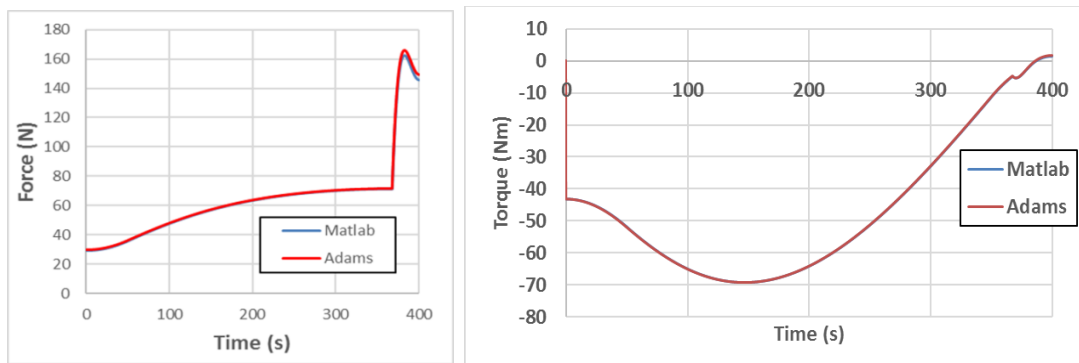


Figure 9 Comparisons between analytical calculations and numerical analysis, (left) Comparison between analytical (MATLAB) and numerical (MSC ADAMS) solutions for reaction force at upper batten, (right) Comparison between analytical (MATLAB) and numerical (MSC ADAMS) solutions for reaction force at upper batten

The linear and angular velocities and the accelerations on point B' (longeron AB', B' rotation point) using the MATLAB code are presented in Figures 10 and 11 respectively:

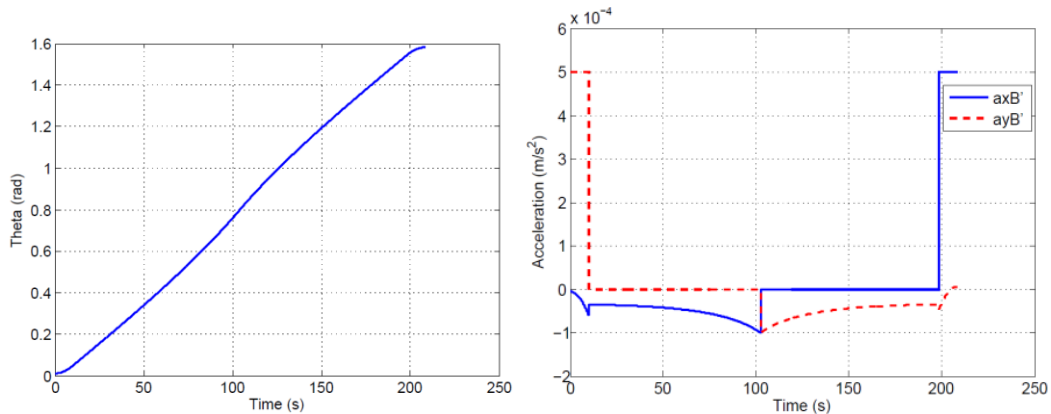


Figure 10: 10 Angle θ versus deployment time, linear accelerations (x-axis, y-axis) for the point B' , (left) Angle θ versus deployment time, (right) (b) Angle θ versus linear accelerations

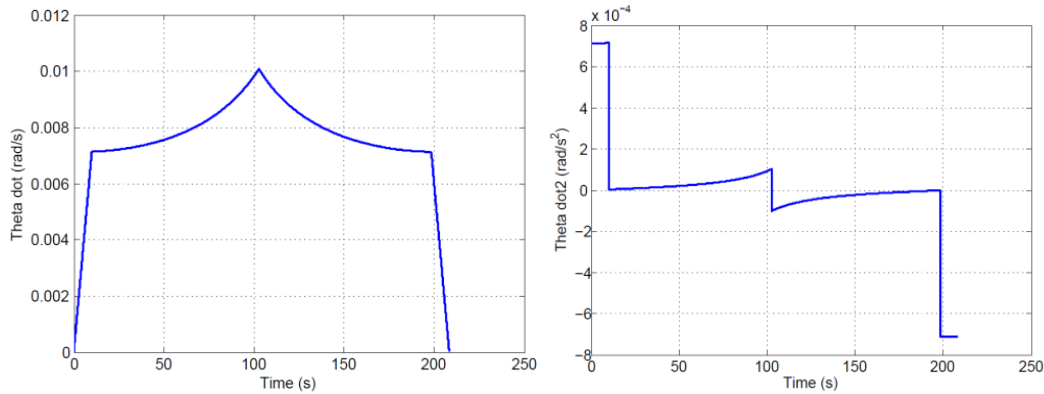


Figure 11: Angular velocity θ' and angular acceleration θ'' versus deployment time for longeron AB', (left) Angular velocity θ' versus deployment time, (right) (b) angular acceleration θ'' versus linear accelerations

As the MSC ADAMS rigid body analysis was performed and calibrated using the numerical MATLAB code, additional flexibility parameters were considered. The longerons' angular velocities and accelerations, inertia loads that applied to the 2D basic module lead to elastic deformations. These deformations could be critical for the early design stage leading to up normal operation violating the acceptance criteria. To simulate the elastic behavior of the 2D basic module, additional (structural) FEA models were developed in collaboration with MSC ADAMS (kinematics/dynamics) models including the battens and longerons normal modes (eigenfrequencies/eigenvalues). Both rigid and flexible models in MSC ADAMS are presented in Figure 12 and Figure 13 respectively.

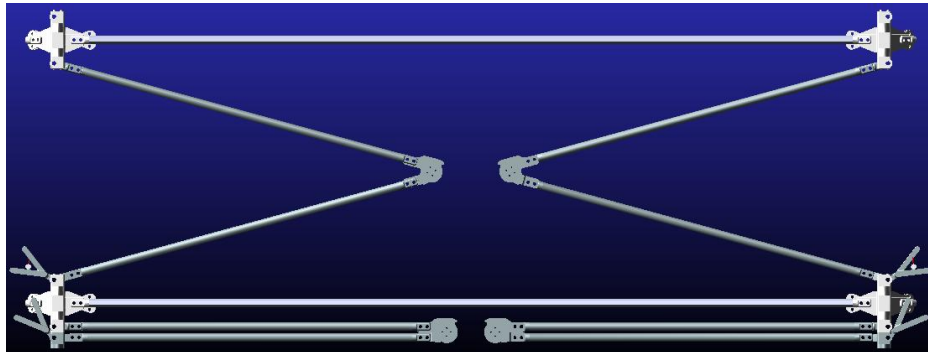


Figure 12: Rigid body model in MSC ADAMS

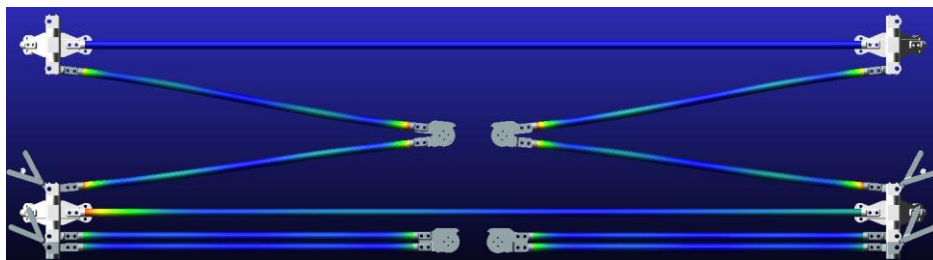


Figure 13: Flexible body model in MSC ADAMS

It was proven that the most demanding phase in terms the loading of truss components was the initial stages of the deployment phase. Once deployed, the loads exerted on the truss due to S/C maneuvers and other operations are very low. Based on the results of the kinematic/dynamics analysis, a procedure was launched including an additional FEM study for the evaluation of the developed loads during deployment. The methodology-procedure included the following steps:

- MSC Adams is used for all the kinematic-dynamic simulations; appropriate boundary conditions and properties are used to simulate the motion; All parts are considered as rigid.
- The 2D basic module members (longeron and battens) are considered as flexible bodies in NX Nastran including the stiffness data (Elasticity modulus, Poisson ratio etc.) . These bodies were included on the MSc ADAMS software, repeating the kinematics-dynamics analysis. Initial evaluation check between rigid and flexible body results.

- The forces and the moments' profiles from the flexible-body kinematic/dynamics analysis that correspond on deployment loads were set as an Loads output.
- The Load Output file was imported to NX Nastran, where a Linear/non-linear static analysis (inertia relief ON) was performed, calculating the stress-displacement field on the 2D basic module's elements. Final evaluation check between rigid and flexible body.

The results of a static analysis with inertia relief for a longeron (the CFRP part) for the maximum actuation torque during deployment (around 43°) and maximum cable tension conditions are presented in Figure 14. Deformed geometry is plotted against the undeformed state. Contours correspond to the Hill failure index for the longeron modelled with shell laminate elements.

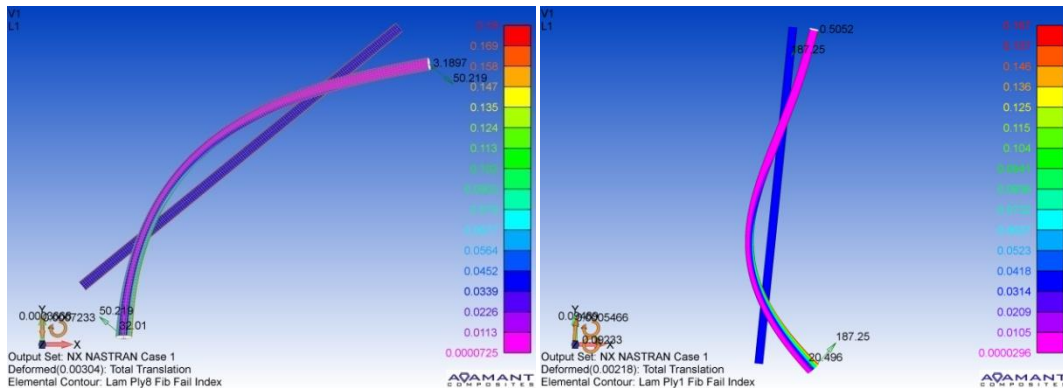


Figure 14: Deformation and failure index for the Longeron CFRP tube at the point of maximum torque and Deformation and failure index for the Longeron CFRP tube at the point of maximum cable tension (left) Deformation and failure index for the Longeron CFRP tube at the point of maximum torque, (right) Deformation and failure index for the Longeron CFRP tube at the point of maximum cable tension

A detailed FEA model was also developed for the complete longeron sub-assembly including the actuation lever, end fittings and part of the mid-longeron mechanism. The most stressed areas were investigated for the possibility of failure. The case study analysis for the maximum torque application is presented in Figure 15 where a peak-stress on the longeron connector was observed. The comparison between the rigid and the flexible body is presented in Figure 16 and the difference on the button's position was investigated for the deployment time.

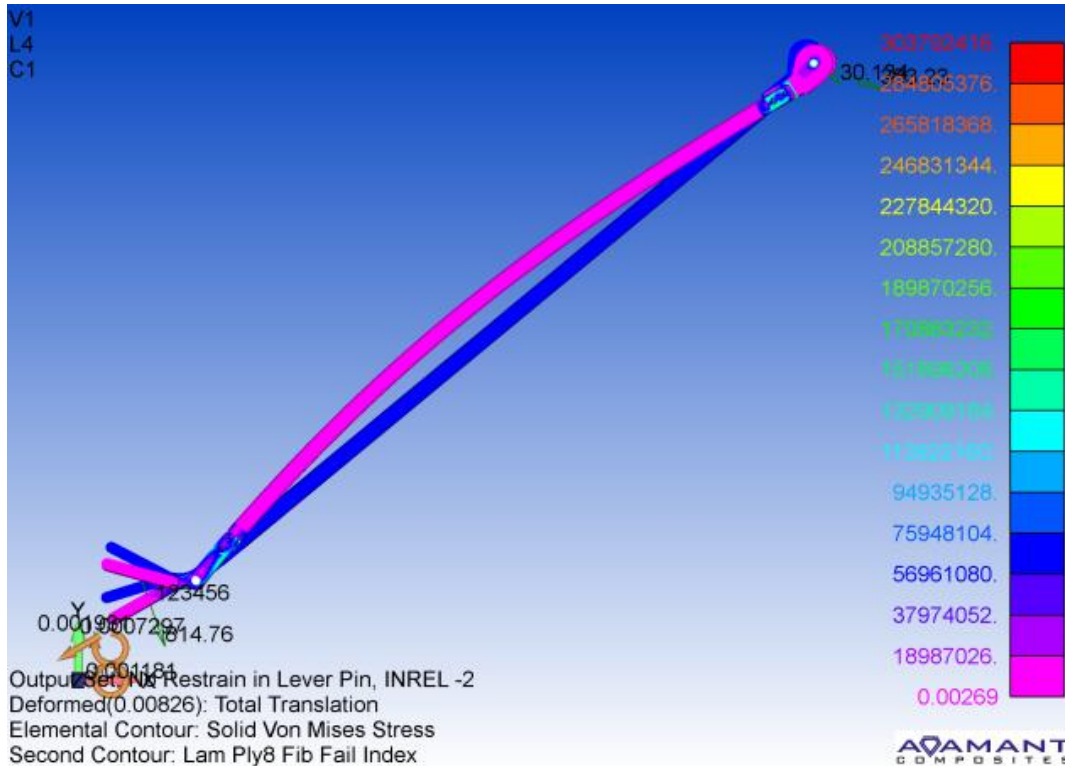


Figure 15: Deformed body and Von-Mises stress for the half longeron sub-assembly (peak stress 304 MPa) for Maximum actuation torque scenario.

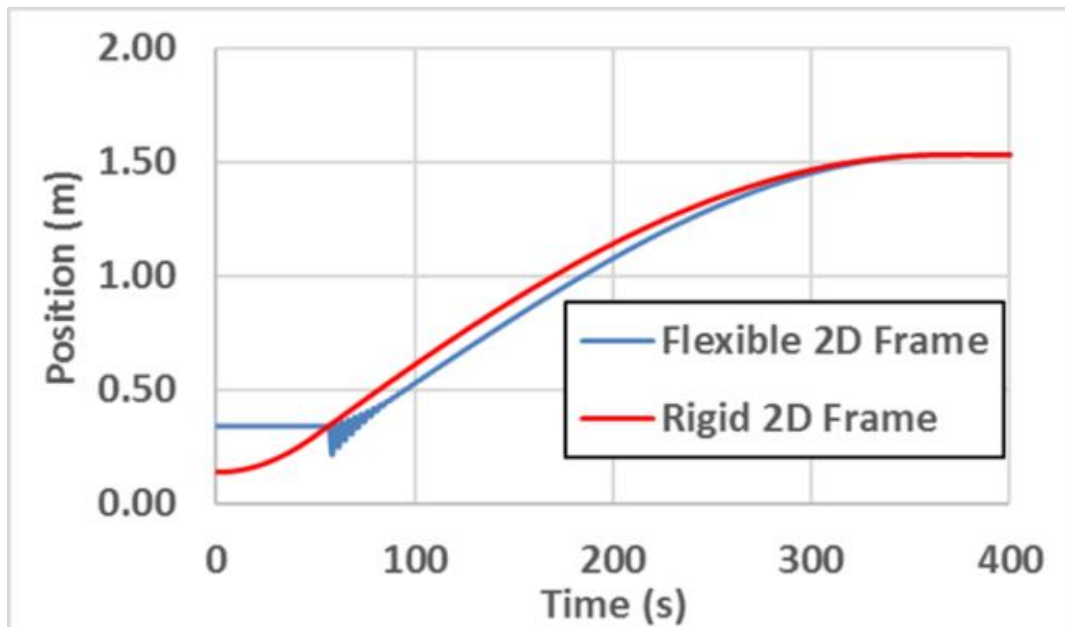


Figure 16: Upper batten position comparison between rigid and flexible body analyses.

The oscillations at the beginning of the deployment procedure were observed as a major risk. Substructures-attachments were developed increasing the structural damping during the early stages of deployment process ($t < 100s$) securing the successful operation.

IV. CONCLUSIONS

In this survey, a MATLAB code was developed using analytical equations for the kinematic and dynamic simulation of the 2D basic module of ESA-LAGARD mast. This simulation was used for the verification of MSC-ADAMS model (both rigid and flexible body analysis) and for the contact parameters' calibration. The results between MATLAB numerical code and MSC ADAMS software are in excellent

agreement for rigid body assumptions permitting the successful calibration of the contact parameters. Furthermore, the simulation of flexibility effects via MSC ADAMS provides useful results for the 2D basic module optimization process. Moreover, these results are useful for the Testing plan establishment and the ground support equipment process overview where the prototype structure of a 2D basic module will experience the deployment loads.

For future work, the 2D basic module has to pass the a) : gravity off loading test, b)the gravity of loading test including thermal effects and c) the MATLAB code will be upgraded to include thermal and nonlinear friction effect for additional comparisons between numerical models and tests.

ACKNOWLEDGMENTS

The authors wish to acknowledge : Dr A. Vavouliotis (Managing Director, Adamant Composites Ltd) and Mr. D. Lamprou (Systems Engineer, Adamant Composites Ltd) for the opportunity to participate in ESA-LAGARD project's design and development phases. Special thanks to all the colleagues and friends (both UPat-AML and Adamant Composites Ltd) for their valuable assistance and the excellent collaboration all these years.

REFERENCES

- [1]. A review on large deployable structures for astrophysics missions, L. Puig et al., 2010
- [2]. Advances in deployable structures and surfaces for large apertures in space, J. Santiago-Prowald et al., 2013
- [3]. Modeling and analysis of a large deployable antenna structure, Z. Chu et al., 2014
- [4]. Dynamic analysis of the deployment for mesh reflector deployable antennas with the cable-net structure, Y. Zhang et al., 2017
- [5]. Deployment analysis and control of deployable space antenna, L. Tuanjie, 2012
- [6]. Deployment analysis considering the cable-net tension effect for deployable antennas, Y. Zhang, 2016
- [7]. Theoretical analysis and experiments of a space deployable truss structure, R. Zhang et al., 2014
- [8]. MATLAB for Engineers, H. Moore, 2014
- [9]. Vector Mechanics for Engineers: Dynamics, F. P. Beer et al, 2015
- [10]. MSC ADAMS view help, MSC ADAMS, 2016
- [11]. Space Vehicle Mechanisms: Elements of Successful Design, Conley, 1998
- [12]. LAGARD Project Technical Note TN2100: Design and Analysis, Adamant Composites Ltd, 2016

Evangelos Kaslis, et. al. "Kinematic & Dynamic Simulation Of A 2d Aerospace Structure for Esa - Lagard Project." *The International Journal of Engineering and Science (IJES)*, 10(12), (2021): pp. 11-22.